Steady States of Infinite-Size Dissipative Quantum Chains via Imaginary Time Evolution

Adil A. Gangat,[1] Te I,[1] and Ying-Jer Kao[1,2,*]
[1]Department of Physics, and Center for Theoretical Sciences, National Taiwan University, Taipei 10607, Taiwan
[2]National Center for Theoretical Sciences, National Tsing Hua University, Hsinchu 30013, Taiwan
(Received 31 August 2016; published 5 July 2017)

Directly in the thermodynamic limit, we show how to combine local imaginary and real-time evolution of tensor networks to efficiently and accurately find the nonequilibrium steady states (NESSs) of one-dimensional dissipative quantum lattices governed by a local Lindblad master equation. The imaginary time evolution first bypasses any highly correlated portions of the real-time evolution trajectory by directly converging to the weakly correlated subspace of the NESS, after which, real-time evolution completes the convergence to the NESS with high accuracy. We demonstrate the power of the method with the dissipative transverse field quantum Ising chain. We show that a crossover of an order parameter shown to be smooth in previous finite-size studies remains smooth in the thermodynamic limit.

DOI: 10.1103/PhysRevLett.119.010501

Introduction.—The out-of-equilibrium behavior of dissipative many-body systems is of relevance to experimental platforms such as trapped ions [1], cold atoms [2], superconducting circuits [3–5], and nanoelectromechanical systems [6]. Theoretical activity has recently increased around developing numerical methods for determining the nonequilibrium steady states (NESSs) of such dissipative lattices [7–15]. This includes tensor network methods [16–19], which serve as an efficient numerical ansatz for states that obey an area law [20] (i.e., have small correlations between their bipartitions). It is proved that the mutual information of the NESS of a local dissipative quantum system satisfies an area law [21,22], assuring that their tensor network representation, if found, will be computationally efficient. Also, a proof for the stability [23] of NESSs against local system perturbations assures that theoretically determined NESSs of translationally invariant systems are of relevance to experiments, where translational invariance can only be approximate.

The focus of the present work is on the problem of numerically finding the tensor network representation of the NESSs of translationally invariant one-dimensional systems in the thermodynamic limit. The infinite-size version of the time-evolving block decimation (iTEBD) algorithm [24] enables a (local) time evolution directly in the thermodynamic limit using a matrix product state (MPS) that spans only a single unit cell of the target state. Also, the iTEBD algorithm can efficiently be used for both imaginary and real-time evolution with local operators and is technically simple to implement.

When imaginary time evolution is performed with a Hamiltonian, the fixed point lies in the ground state manifold of the given Hamiltonian. An efficient tensor network can accommodate the entire imaginary time evolution trajectory if the fixed point obeys an area law. Furthermore, the convergence toward the fixed point is exponentially fast with a rate proportional to the energy gap of the Hamiltonian. Therefore, imaginary time evolution with iTEBD is a very efficient way to obtain ground states of local Hamiltonians in the thermodynamic limit.

For real-time evolution of dissipative systems, the fixed point lies in the NESS manifold. However, real-time evolution with iTEBD [25] is not always an efficient way to obtain the NESS, since portions of the real-time evolution trajectory from the initial state to the NESS may not obey an area law even when the NESS does so itself [9]. Further, the rate of convergence to the NESSs may be very slow [11,26]. For finite-size chains, recent works [9,11] tackle these problems using variational methods. These approaches, though accurate, cannot be easily generalized to infinite-size systems and are not technically so simple to implement. A method that instead uses local imaginary time evolution with iTEBD would overcome the shortcomings of these real-time evolution and variational search methods.

Prior approaches to finding one-dimensional NESSs with tensor networks have exploited the area law property of the target state to achieve efficiency. By additionally exploiting a closely related but distinct physical property, exponential decay of two-point correlators, we here show how to overcome the limitations of real-time evolution and variational searches for the NESS: we construct an auxiliary local Hamiltonian such that its ground state approximates the NESS and perform iTEBD imaginary time evolution with the auxiliary Hamiltonian. In this way, we are able to bypass any highly correlated portions of the real-time evolution trajectory and arrive in the area-law-obeying neighborhood of the NESS exponentially quickly. We then further improve the convergence to the NESS using a real-time evolution with the Lindbladian.

The auxiliary Hamiltonian approach that we present holds potential for the thermodynamic limit of higher-dimensional dissipative systems as well, since both imaginary time evolution and variational optimization [27] have been demonstrated to obtain ground states with the higher-dimensional tensor network ansatz of infinite-size projected entangled pair states (iPEPS) [28].

As a demonstration of our method, we use it to probe the thermodynamic limit of a crossover in an order parameter

of the one-dimensional dissipative transverse field Ising model. To our knowledge, non-mean-field studies of this crossover have only previously been performed in the finite-size limit. Our result shows that this crossover remains smooth in the thermodynamic limit.

Method.—The equation of motion for a (discrete) quantum system coupled to a Markovian environment is given by the Lindblad master equation (LME) [29]. Under the Choi isomorphism ($\hat{\rho} = \sum_j p_j |\Psi_j\rangle\langle\Psi_j| \rightarrow |\rho\rangle = \sum_j p_j |\Psi_j\rangle \otimes |\Psi_j\rangle$), the LME is

$$\frac{d}{dt}|\rho\rangle = \hat{\mathcal{L}}|\rho\rangle, \tag{1}$$

with

$$\hat{\mathcal{L}} = -\frac{i}{\hbar}(H \otimes \mathbb{1} - \mathbb{1} \otimes H^T) + \sum_\alpha \frac{1}{2}(2L_\alpha \otimes \bar{L}_\alpha - L_\alpha^\dagger L_\alpha \otimes \mathbb{1} - \mathbb{1} \otimes L_\alpha^T \bar{L}_\alpha), \tag{2}$$

where H is the system Hamiltonian and L_α are dissipative operators.

A matrix product density operator (MPDO) [30] is a tensor network that serves as an efficient ansatz for a mixed state density matrix of a one-dimensional lattice when the correlations between real space bipartitions of the state are small [30,31]. Under the Choi isomorphism, the MPDO [30] can be written as a MPS [32]: $|\rho\rangle = \sum_{s_1,\ldots,s_N=1}^{d} \mathrm{Tr}(A_1^{s_1} \ldots A_N^{s_N})|s_1 \ldots s_N\rangle$, where the A_j are tensors of dimension $d \times D \times D$, and D is referred to as the "bond dimension." The chief advantage of such an ansatz is that while D needs to be exponentially large in the system size for the MPS to be exact, a much smaller (i.e., computationally tractable) value of D yields extremely high accuracy for states that obey an area law [20]. Another advantage of this ansatz is that the entanglement spectrum (denoted λ_i^2 below) between sub-blocks of any bipartition of the lattice is readily calculated [33]. In the case of infinite-size systems with translational invariance, the MPDO is referred to as an "iMPDO," and it can span a Hilbert space as small as a single unit cell of the target physical state [24].

The NESSs (denoted $|\rho_\infty\rangle$) of dissipative systems described by the LME are defined by $\hat{\mathcal{L}}|\rho_\infty\rangle = 0$, with the constraint that the $|\rho_\infty\rangle$ are vectorized forms of positive operators with unit trace (i.e., physically valid density matrices; see below for further discussion). The authors of Ref. [9] observe that $|\rho_\infty\rangle$ will also be the ground state of the *nonlocal* Hamiltonian $\hat{\mathcal{L}}^\dagger\hat{\mathcal{L}}$. For finite-size chains, they present a variational method for finding the (nondegenerate) ground state of $\hat{\mathcal{L}}^\dagger\hat{\mathcal{L}}$ as a way of determining $|\rho_\infty\rangle$. However, their method does not apply directly (i.e., without costly extrapolation from finite-size scaling) in the thermodynamic limit. Since $\hat{\mathcal{L}}^\dagger\hat{\mathcal{L}}$ is nonlocal, imaginary time evolution with iTEBD also cannot be used to find its ground state. Here we show that it is possible to construct a *local* auxiliary Hamiltonian $\mathcal{H}$ such that the iTEBD algorithm may be used to approach the infinite-size NESSs via imaginary time evolution:

$$|\rho_\infty\rangle \approx \lim_{\tau\rightarrow\infty} \frac{\exp(-\mathcal{H}\tau)|\rho_0\rangle}{\|\exp(-\mathcal{H}\tau)|\rho_0\rangle\|}, \tag{3}$$

where $|\rho_0\rangle$ is any vectorized density matrix such that $\langle\rho_\infty|\rho_0\rangle \neq 0$.

As an initial motivation, we observe that if F is a *local* Hamiltonian with positive eigenvalues, F^2 will be a *nonlocal* Hamiltonian with the same ground and excited states as the local F. This suggests the possibility of finding a local Hamiltonian $\mathcal{H}$ whose ground state is at least a good approximation to the ground state of the nonlocal $\hat{\mathcal{L}}^\dagger\hat{\mathcal{L}}$.

We assume that $\hat{\mathcal{L}}$ is a translationally invariant local operator; this corresponds to the case of a translationally invariant local system Hamiltonian H and translationally invariant local dissipation operators L_α. $\hat{\mathcal{L}}$ can, therefore, be expressed as a sum of translationally invariant local terms ($\hat{\mathcal{L}} = \sum_{r\epsilon\mathbb{Z}} \hat{\mathcal{L}}_r$), and we may write

$$\hat{\mathcal{L}}^\dagger\hat{\mathcal{L}} = \sum_{r,s\epsilon\mathbb{Z}} \hat{\mathcal{L}}_r^\dagger\hat{\mathcal{L}}_s. \tag{4}$$

We may use $\langle\hat{\mathcal{L}}_r\rangle = 0$ as a benchmark and $|\langle\hat{\mathcal{L}}_r\rangle|$ as a figure of merit. It was analytically proven in Ref. [21] that the two-point correlator shows an exponential decay in a NESS. Also, $|\rho_\infty\rangle$ is determined completely by $\hat{\mathcal{L}}$, which is local. Therefore, the long-range couplings in $\hat{\mathcal{L}}^\dagger\hat{\mathcal{L}}$ do not play a significant role in determining its ground state $|\rho_\infty\rangle$, and we may truncate the second sum in Eq. (4) by setting $s = r$. This truncation preserves both Hermiticity and positivity. Further, taking the kth root of each remaining term, we arrive at the proposed local auxiliary Hamiltonian for imaginary time evolution to the NESS:

$$\mathcal{H} = \sum_{r\epsilon\mathbb{Z}} (\hat{\mathcal{L}}_r^\dagger\hat{\mathcal{L}}_r)^{1/k}. \tag{5}$$

If the (numerical) gap between the lowest two eigenvalues of $\hat{\mathcal{L}}_r^\dagger\hat{\mathcal{L}}_r$ is less than 1, $k > 1$ will increase the gap since $\hat{\mathcal{L}}_r^\dagger\hat{\mathcal{L}}_r$ is positive semidefinite. This will yield faster convergence toward the ground state of $\mathcal{H}$ (for imaginary time evolution, the rate of convergence is proportional to the gap). While $\mathcal{H}$ for $k > 1$ will not generally commute with $\mathcal{H}$ for $k = 1$, we find that the advantage gained (see next section) outweighs this drawback.

The form of $\hat{\mathcal{L}}_r$ can change as long as $\hat{\mathcal{L}} = \sum_{r\epsilon\mathbb{Z}} \hat{\mathcal{L}}_r$. $\hat{\mathcal{L}}_r$ with larger support leads to longer-range couplings in $\mathcal{H}$; for $\hat{\mathcal{L}}_r$ of infinite support, $\mathcal{H}$ becomes equal to $\hat{\mathcal{L}}^\dagger\hat{\mathcal{L}}$ (when $k = 1$). We may, therefore, decrease the distance between $|\rho_\infty\rangle$ and the ground state of $\mathcal{H}$ by increasing the support of $\hat{\mathcal{L}}_r$, albeit with an increased computational cost.

Rather than relying on imaginary time evolution alone, the following hybrid method can be more efficient: with small D, relatively large time step, and $\hat{\mathcal{L}}_r$ of small support, imaginary time evolution can be used to rapidly converge to the area-law-obeying neighborhood of the NESS, after which real-time evolution with iTEBD can minimize $|\langle\hat{\mathcal{L}}_r\rangle|$ with successively smaller time steps and successively larger D. The Trotter error of iTEBD vanishes polynomially in the time step size, and the spectrum (λ_i^2) decays roughly exponentially when there is an area law.

As mentioned, for the converged solution to be physically valid, it must correspond to a positive operator. If the NESS is unique, it is discussed in Ref. [9] that this requirement is automatically satisfied when $\hat{\mathcal{L}}|\rho\rangle = 0$ because $\hat{\mathcal{L}}$ is a completely positive map. We may, therefore, assume a unique NESS and assure (near) positivity by attaining very small $|\langle\hat{\mathcal{L}}_r\rangle|$ and converging the spectrum. This is similar to what is done in Ref. [9], which assures (near) positivity by variationally reducing $\langle\hat{\mathcal{L}}^\dagger\hat{\mathcal{L}}\rangle$ to below a chosen threshold and converging various observables, and Ref. [11], which assures (near) positivity by variationally minimizing $\|\hat{\mathcal{L}}|\rho\rangle\|$.

Numerical results.—There have been various numerical investigations of the 1D quantum Ising model with nearest-neighbor coupling, uniform transverse magnetic field, and on-site dissipation [2,9,26,34–44]. Here we look at the following incarnation: the system is governed by Eqs. (1) and (2) with the Hamiltonian given by $H = \sum_{j\epsilon\mathbb{Z}} H_j$, where ($\hbar = 1$),

$$H_j = \sigma_z^{[j]}\sigma_z^{[j+1]} + h_x\sigma_x^{[j]}, \tag{6}$$

j is the lattice site index, and h_x is the transverse field strength; the local dissipation terms are given by $L_j = \sqrt{\gamma}\sigma_-^{[j]}$, where γ is a decay rate from spin-up to spin-down.

We choose a tensor network that is structured such that two physical sites are associated to each of the numerical sites of a two-site iMPDO. For both imaginary and real-time evolution, a fourth order Suzuki-Trotter expansion of the evolution operators is used. For the imaginary time evolution, we choose the following 4-local form ($\hbar = 1$) for $\hat{\mathcal{L}}_r$:

$$\begin{aligned}\hat{\mathcal{L}}_r &= -i(H_r\otimes\mathbb{1} - \mathbb{1}\otimes H_r^T) + \frac{1}{2}\mathrm{diss}[2r] + \frac{1}{2}\mathrm{diss}[2r+1] \\ &\quad + \frac{1}{2}\mathrm{diss}[2r+2] + \frac{1}{2}\mathrm{diss}[2r+3], \\ H_r &= \frac{1}{2}\sigma_z^{[2r]}\sigma_z^{[2r+1]} + \sigma_z^{[2r+1]}\sigma_z^{[2r+2]} + \frac{1}{2}\sigma_z^{[2r+2]}\sigma_z^{[2r+3]} \\ &\quad + \frac{1}{2}h_x(\sigma_x^{[2r]} + \sigma_x^{[2r+1]} + \sigma_x^{[2r+2]} + \sigma_x^{[2r+3]}),\end{aligned} \tag{7}$$

where the local dissipation term is given as $\mathrm{diss}[r] = (\gamma/2)(2\sigma_-^{[r]}\otimes\sigma_-^{[r]} - \sigma_+^{[r]}\sigma_-^{[r]}\otimes\mathbb{1}^{[r]} - \mathbb{1}^{[r]}\otimes\sigma_+^{[r]}\sigma_-^{[r]})$. The overlap between $\hat{\mathcal{L}}_r$ and $\hat{\mathcal{L}}_{r+1}$ in this form is two sites; forms resulting in three site overlap would yield more intersite couplings in $\mathcal{H}$ and, therefore, a better match between the ground state of $\mathcal{H}$ and $|\rho_\infty\rangle$, but the above form is numerically more efficient and sufficient for our demonstration. It is straightforward to verify that this form satisfies $\hat{\mathcal{L}} = \sum_{r\epsilon\mathbb{Z}}\hat{\mathcal{L}}_r$.

For the finite-size version of this model, a previous numerical study [38] shows that a smooth crossover occurs in the value of the up-spin density $n_\uparrow = \sum_r\langle\hat{n}_\uparrow^{[r]}\rangle/N$ as h_x/γ is increased from small to large values. To demonstrate the theoretical validity of the imaginary time method put forth in the previous section, we probe this crossover (for $\gamma = 0.5$) in the thermodynamic limit with imaginary time evolution and real-time evolution independently. The purpose here is to demonstrate that the imaginary time method can come close to the NESS very efficiently and robustly (i.e., with very crude parameters and convergence). In the Supplemental Material [45], we check the convergence of the imaginary time evolution vs both D and imaginary time step size at the middle of the crossover. From there, we determine that fixing $D = 15$, and the imaginary time step size at $d\tau = 10^{-2}$ (in units of the inverse Ising interaction strength squared) is sufficient for this purpose. For real-time evolution, we also use a time step size of $dt = 10^{-2}$ (in units of inverse Ising interaction strength). The simulations are run until the spectrum is converged according to the following criterion: $|\lambda_1(t+\Delta t) - \lambda_1(t)|/\lambda_1(t+\Delta t) < 10^{-7}$, where λ_1 is the largest singular value in the iMPDO. At each value of h_x, the same initial state is used for both imaginary time and real-time evolution. The results are illustrated in Fig. 1. The spectra in the middle panel show that the imaginary time evolution ($k = 4$) and the real-time evolution have converged to a weakly correlated subspace. The bottom panel shows that $|\langle\hat{\mathcal{L}}_r\rangle|$ is much smaller than the smallest energy scale in $\hat{\mathcal{L}}_r$ for real-time evolution and imaginary time evolution (when $k = 4$). The results in these two panels indicate proximity to the NESS. Because $|\langle\hat{\mathcal{L}}_r\rangle|$ is smallest for real-time evolution, the data in the top panel for the real-time evolution can be considered the most accurate, and the increasing overall match between the imaginary time data and real-time data for $n_\uparrow$ with higher k shows that the accuracy of the imaginary time evolution improves with larger k. Though we do not investigate it here, it is possible that the significant enhancement in accuracy with larger k is due to the removal of metastability [46,47]. Taken together, these results demonstrate the conceptual validity of the imaginary time evolution method as an alternative to real-time evolution for approaching the state space neighborhood of the NESS. The level of accuracy achieved with the imaginary time method is remarkable given the crude convergence scheme and enormous truncation of $\hat{\mathcal{L}}^\dagger\hat{\mathcal{L}}$ in forming $\mathcal{H}$. The physical explanation for the success of the truncation of $\hat{\mathcal{L}}^\dagger\hat{\mathcal{L}}$ is the exponential decay of the two-point correlators in the NESS. For comparison, we show simulation results for a 2-local form of $\hat{\mathcal{L}}_r$ in the Supplemental Material [45].

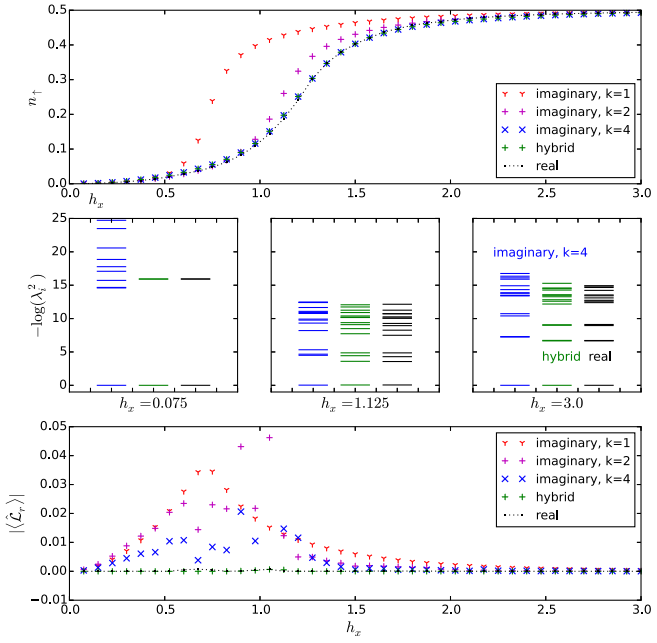

FIG. 1. A comparison of iTEBD imaginary time and iTEBD real-time evolution, and a demonstration of the hybrid method, for an infinite-size Ising chain with Hamiltonian of the form in Eq. (6) and dissipation rate $\gamma = 0.5$ when the spectrum is converged as described in the main text. The results show that imaginary time evolution can serve as an alternative to real-time evolution for approaching the NESS. The imaginary time evolution results are for the 4-local form of $\hat{\mathcal{L}}_r$ given in Eq. (7). (Top) Converged up-spin density $n_\uparrow$ vs transverse magnetic field strength h_x for real-time evolution and different values of k for the imaginary time evolution. The overall accuracy of the imaginary time evolution improves with larger k. (Middle) Entanglement spectra after convergence for three different values of h_x, with imaginary time evolution results shown for $k = 4$. The rapid decay of the spectra shows that both evolutions converge to a weakly correlated subspace, suggesting proximity to the NESS. The spectra of the hybrid method converge to those of real-time evolution, indicating the hybrid method also arrives at the same NESS. (Bottom) For real time and imaginary time with $k = 4$, $|\langle\hat{\mathcal{L}}_r\rangle|$ converges to values much less than the smallest energy scale in the system, also suggesting proximity to the NESS. The data for the hybrid method indicate that performing real-time evolution after the imaginary time evolution enhances the accuracy as expected.

The 2-local form also permits successful imaginary time evolution toward the NESS but with poorer accuracy.

We note that our results indicate that in this one-dimensional case, the crossover in $n_\uparrow$ remains smooth in the thermodynamic limit; this is in contrast to the sharp transition predicted for the two-dimensional version of the model [8,43]. This is the first study of this crossover in the thermodynamic limit beyond the mean-field theory.

We also demonstrate the functionality of the full hybrid method (imaginary time evolution followed by real-time evolution). For the same system parameters as the other data, the top panel of Fig. 1 shows the converged data from the

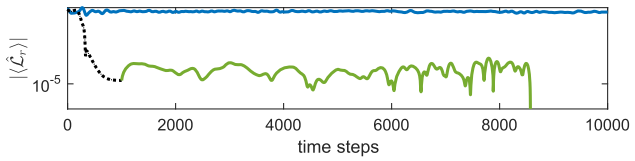

FIG. 2. System parameters: $\gamma = 0.01$, $h_x = 1$. Real-time evolution (upper solid line, blue) with $D = 25$ from the initial state fails to converge to the NESS over a time scale equal to the largest intrinsic time scale of the system. With the hybrid method ($D = 6$), imaginary time evolution (dotted line) rapidly achieves proximity to the NESS, after which, real-time evolution (lower solid line, green) efficiently attains $|\langle\hat{\mathcal{L}}_r\rangle| < 10^{-6}$.

hybrid method when the state at the end of the imaginary time evolution for $k = 4$ is converged to $|\langle\hat{\mathcal{L}}_r\rangle| < 10^{-3}$ with real-time evolution. The entanglement spectra of the hybrid method also converge to those of real-time evolution, indicating both methods reach the same NESS.

To demonstrate that the hybrid method remains efficient where real-time evolution becomes inefficient, with $\gamma = 0.01$ and $h_x = 1$, we evolve a highly correlated initial state with the two methods separately and find that the hybrid method converges rapidly in several minutes of computation time with $D = 6$, while real-time evolution over the same number of time steps becomes trapped in an area-law-violating sector of the Hilbert space even with D as high as 25. The time evolution of $|\langle\hat{\mathcal{L}}_r\rangle|$ is shown in Fig. 2, while the evolution of the spectra and further details are given in the Supplemental Material [45]. It is clear that the initial imaginary time evolution bypasses the highly correlated region of the real-time trajectory and brings the iMPDO close to the neighborhood of the NESS; thus, an efficient real-time evolution becomes possible, and very high accuracy can be achieved.

Discussion.—Imaginary time evolution of tensor networks with iTEBD is an efficient way of approximating the ground states of many-body quantum systems in the thermodynamic limit when an area law holds for the ground state; the area law permits high accuracy with a computationally tractable bond dimension. Here we have shown that imaginary time evolution of an iMPDO with iTEBD is an efficient way of approximating the NESS of dissipative quantum chains when the NESS has both an area law and exponential decay of two-point correlators; the area law permits the iMPDO to approximate the NESS with high accuracy with a computationally tractable bond dimension, and the exponential decay of two-point correlators permits the construction of a *local* auxiliary Hamiltonian with which to perform imaginary time evolution with iTEBD. Real-time evolution can be employed after the imaginary time evolution to efficiently obtain the NESS with very high accuracy. Alternatively, but perhaps less efficiently, imaginary time evolution may be used alone to reach the NESS by converging not only in the time step size and bond dimension but also the support size of the local terms in the auxiliary Hamiltonian.

In the course of demonstrating our method with the dissipative transverse field quantum Ising chain, we have shown that a crossover of an order parameter that is smooth in the finite-size limit remains smooth in the thermodynamic limit, in contrast to the two-dimensional case.

With the higher-dimensional tensor network of iPEPS, both variational optimization and imaginary time evolution have been shown to work [27,28], and real-time evolution toward NESSs was also recently demonstrated [15]; the method presented here may thereby be extended to higher dimensions.

We note that the imaginary time evolution method presented here can also apply to finite-size chains by using TEBD instead of iTEBD, and it would be interesting to compare the performance of the hybrid method in this paper with the variational methods [9,11] for finding the NESSs of finite-size chains.

Y.-J. K. and A. A. G. acknowledge discussions with Ian McCulloch, Roman Orús, and Augustine Kshetrimayum and the hospitality of the Institut für Physik at Johannes Gutenberg-Universität. A. A. G. acknowledges early pedagogical interactions at the University of Queensland with Guifré Vidal and Ho N. Phien regarding MPS and TEBD. We also acknowledge helpful comments by Garnet Chan and Frank Pollmann. We thank Dominic C. Rose for insightful remarks regarding metastability. Some of the simulations were coded using the Uni10 tensor library [48]. This work is supported by the MOST in Taiwan through Grants No. 104-2112-M-002 -022 -MY3 and No. 105-2112-M-002 -023 -MY3.

*yjkao@phys.ntu.edu.tw

[1] P. Schindler, M. Müller, D. Nigg, J. Barreiro, E. Martinez, M. Hennrich, T. Monz, S. Diehl, P. Zoller, and R. Blatt, Nat. Phys. **9**, 361 (2013).
[2] H. Schwager, J. I. Cirac, and G. Giedke, Phys. Rev. A **87**, 022110 (2013).
[3] A. A. Houck, H. E. Türeci, and J. Koch, Nat. Phys. **8**, 292 (2012).
[4] S. Schmidt and J. Koch, Ann. Phys. (Berlin) **525**, 395 (2013).
[5] K. L. Hur, L. Henriet, A. Petrescu, K. Plekhanov, G. Roux, and M. Schiró, C. R. Phys. **17**, 808 (2016).
[6] J. Lozada-Vera, A. Carrillo, O. P. S. Neto, J. K. Moqadam, M. D. LaHaye, and M. C. Oliveira, Europhys. J. Quantum Technol. **3**, 1 (2016).
[7] A. H. Werner, D. Jaschke, P. Silvi, M. Kliesch, T. Calarco, J. Eisert, and S. Montangero, Phys. Rev. Lett. **116**, 237201 (2016).
[8] H. Weimer, Phys. Rev. Lett. **114**, 040402 (2015).
[9] J. Cui, J. I. Cirac, and M. C. Bañuls, Phys. Rev. Lett. **114**, 220601 (2015).
[10] S. Finazzi, A. Le Boité, F. Storme, A. Baksic, and C. Ciuti, Phys. Rev. Lett. **115**, 080604 (2015).
[11] E. Mascarenhas, H. Flayac, and V. Savona, Phys. Rev. A **92**, 022116 (2015).
[12] A. Dorda, M. Ganahl, H. G. Evertz, W. von der Linden, and E. Arrigoni, Phys. Rev. B **92**, 125145 (2015).
[13] M. Raghu, C. D. Freeman, S. Mumford, N. Tubman, and B. Swingle, arXiv:1608.05074.
[14] J. Jin, A. Biella, O. Viyuela, L. Mazza, J. Keeling, R. Fazio, and D. Rossini, Phys. Rev. X **6**, 031011 (2016).
[15] A. Kshetrimayum, H. Weimer, and R. Orús, arXiv:1612.00656.
[16] U. Schollwöck, Ann. Phys. (Amsterdam) **326**, 96 (2011).
[17] F. Verstraete, V. Murg, and J. I. Cirac, Adv. Phys. **57**, 143 (2008).
[18] J. I. Cirac and F. Verstraete, J. Phys. A **42**, 504004 (2009).
[19] R. Orús, Ann. Phys. (Amsterdam) **349**, 117 (2014).
[20] J. Eisert, M. Cramer, and M. B. Plenio, Rev. Mod. Phys. **82**, 277 (2010).
[21] F. G. Brandao, T. S. Cubitt, A. Lucia, S. Michalakis, and D. Perez-Garcia, J. Math. Phys. (N.Y.) **56**, 102202 (2015).
[22] R. Mahajan, C. D. Freeman, S. Mumford, N. Tubman, and B. Swingle, arXiv:1608.05074.
[23] T. S. Cubitt, A. Lucia, S. Michalakis, and D. Perez-Garcia, Commun. Math. Phys. **337**, 1275 (2015).
[24] G. Vidal, Phys. Rev. Lett. **98**, 070201 (2007).
[25] R. Orús and G. Vidal, Phys. Rev. B **78**, 155117 (2008).
[26] Z. Cai and T. Barthel, Phys. Rev. Lett. **111**, 150403 (2013).
[27] P. Corboz, Phys. Rev. B **94**, 035133 (2016).
[28] J. Jordan, R. Orús, G. Vidal, F. Verstraete, and J. I. Cirac, Phys. Rev. Lett. **101**, 250602 (2008).
[29] H.-P. Breuer and F. Petruccione, *The Theory of Open Quantum Systems* (Oxford University Press, New York, 2002).
[30] F. Verstraete, J. J. García-Ripoll, and J. I. Cirac, Phys. Rev. Lett. **93**, 207204 (2004).
[31] M. Zwolak and G. Vidal, Phys. Rev. Lett. **93**, 207205 (2004).
[32] D. Perez-Garcia, F. Verstraete, M. M. Wolf, and J. I. Cirac, Quantum Inf. Comput. **7**, 401 (2007).
[33] G. Vidal, Phys. Rev. Lett. **93**, 040502 (2004).
[34] P. Werner, K. Völker, M. Troyer, and S. Chakravarty, Phys. Rev. Lett. **94**, 047201 (2005).
[35] P. Werner, M. Troyer, and S. Sachdev, J. Phys. Soc. Jpn. **74**, 67 (2005).
[36] S. Yin, P. Mai, and F. Zhong, Phys. Rev. B **89**, 094108 (2014).
[37] P. P. Orth, I. Stanic, and K. Le Hur, Phys. Rev. A **77**, 051601 (2008).
[38] A. Hu, T. E. Lee, and C. W. Clark, Phys. Rev. A **88**, 053627 (2013).
[39] C. Ates, B. Olmos, J. P. Garrahan, and I. Lesanovsky, Phys. Rev. A **85**, 043620 (2012).
[40] T. E. Lee, H. Häffner, and M. C. Cross, Phys. Rev. A **84**, 031402 (2011).
[41] C. Joshi, F. Nissen, and J. Keeling, Phys. Rev. A **88**, 063835 (2013).
[42] M. Marcuzzi, E. Levi, S. Diehl, J. P. Garrahan, and I. Lesanovsky, Phys. Rev. Lett. **113**, 210401 (2014).
[43] H. Weimer, Phys. Rev. A **91**, 063401 (2015).
[44] D. C. Rose, K. Macieszczak, I. Lesanovsky, and J. P. Garrahan, Phys. Rev. E **94**, 052132 (2016).
[45] See Supplemental Material at http://link.aps.org/supplemental/10.1103/PhysRevLett.119.010501 for the convergence test of the bond dimension and time steps and a comparison of the real-time evolution and hybrid method.
[46] D. C. Rose (private communication).
[47] K. Macieszczak, M. Guţă, I. Lesanovsky, and J. P. Garrahan, Phys. Rev. Lett. **116**, 240404 (2016).
[48] Y.-J. Kao, Y.-D. Hsieh, and P. Chen, J. Phys. Conf. Ser. **640**, 012040 (2015); http://uni10.org.